

# Generation of Antifouling Layers on Stainless Steel Surfaces by Plasma-Enhanced Crosslinking of Polyethylene Glycol

Baiyan Dong,<sup>1-3</sup> Sorin Manolache,<sup>1</sup> Eileen B. Somers,<sup>3</sup> Amy C. Lee Wong,<sup>2,3</sup> Ferencz S. Denes<sup>1,3,4</sup>

<sup>1</sup>Center for Plasma-Aided Manufacturing, University of Wisconsin-Madison, Madison, Wisconsin

<sup>2</sup>Department of Food Microbiology and Toxicology, University of Wisconsin-Madison, Madison, Wisconsin

<sup>3</sup>Food Research Institute, University of Wisconsin-Madison, Madison, Wisconsin

<sup>4</sup>Department of Biological Systems Engineering, University of Wisconsin-Madison, Madison, Wisconsin

Received 1 November 2004; accepted 3 December 2004

DOI 10.1002/app.21766

Published online in Wiley InterScience (www.interscience.wiley.com).

**ABSTRACT:** Polyethylene glycol (PEG) structures were deposited onto stainless steel (SS) surfaces by spin coating and argon radio frequency (RF)-plasma mediated crosslinking. Electron spectroscopy for chemical analysis (ESCA) and attenuated total reflectance Fourier transform infrared spectroscopy (ATR-FTIR) indicated the presence of  $-\text{CH}_2-\text{CH}_2-\text{O}-$  structure and C-C-C linkage, as a result of the plasma crosslinking, on PEG-modified SS surfaces. Scanning electron microscopy (SEM) indicated complete deposition, and water contact angle analysis revealed higher hydrophilicity on PEG-modified surfaces compared to unmodified SS surfaces. Surface morphology and roughness analysis by atomic force microscopy (AFM) revealed smoother SS sur-

faces after PEG modification. The evaluation of antifouling ability of the PEG-modified SS surfaces was carried out. Compared to the unmodified SS, PEG-modified surfaces showed about 81–96% decrease in *Listeria monocytogenes* attachment and biofilm formation ( $p < 0.05$ ). This cold plasma mediated PEG crosslinking provided a promising technique to reduce bacterial contamination on surfaces encountered in food-processing environments. © 2005 Wiley Periodicals, Inc. *J Appl Polym Sci* 97: 485–497, 2005

**Key words:** poly(ethylene glycol); biofilm; stainless steel; *Listeria monocytogenes*; cold plasma

## INTRODUCTION

Biofilms can be generally defined as cells immobilized on a substratum and often embedded in a matrix of extracellular polymers produced by the microorganisms. Considered ubiquitous in aqueous environments, biofilm formation is a well-recognized phenomenon in food and medical industries and often leads to undesirable effects. In the food processing industry, biofilms formed on surfaces of processing equipment, pipelines, and conveyor systems can result in reduced heat transfer, energy loss, increased fluid frictional resistance, and accelerated corrosion.<sup>1-3</sup> More importantly, biofilms may cause cross contamination of food products, leading to decreased food quality and transmission of foodborne diseases.<sup>4,5</sup> Adherence of microorganisms to implanted polymer or metal surfaces and subsequent colonization on the exposed surfaces are the major initial steps of foreign-body infections.<sup>6</sup> Strategies oriented to minimize bacterial contamination or biofilm-associated infections are highly desirable.

The mechanism of biofilm formation is not completely understood; several factors, including the organisms present, material surface, and the surrounding biological environment, are considered important. When a material is placed in liquid, proteins and other macromolecules are rapidly adsorbed onto the surface followed by reversible bacterial attachment.<sup>7,8</sup> Any surface that can prevent the attachment of proteins and bacteria may retard or inhibit biofilm formation. It has been demonstrated that coating surfaces with hydrophilic polymers resulted in reducing protein and cell adsorption on a variety of surfaces. Most of the research in this area involved poly(ethylene glycol) (PEG) or its derivatives.<sup>9-13</sup>

PEG (or PEO when the molecular weight is larger than 10,000 Daltons), composed of  $-\text{CH}_2-\text{CH}_2-\text{O}-$  repeating units, is highly water soluble and the chains are very flexible. The mechanisms of the antifouling ability of PEG are not fully elucidated. PEG-modified surfaces have been prepared by a number of approaches, including physical adsorption and entrapment, covalent grafting, photo-induced grafting, high-energy radiation grafting, and glow-discharge mediated grafting.<sup>10,14-17</sup> Significantly reduced protein, platelet, and bacterial adsorption and enhanced biocompatibility have been reported on PEG-containing

Correspondence to: F. S. Denes (denes@engr.wisc.edu).

surfaces.<sup>12,18–20</sup> Physical adsorption is the simplest way to achieve PEG-containing surfaces, but it is not the most reliable because of the high solubility of PEG in water. Covalent bonding of PEG to substrates provides stable PEG surfaces, but all of the methods used to graft PEG to surfaces require functional groups to be introduced either on the substrate surface or to the PEG hydroxyl group. Moreover, these often require complex processes or usage of large amounts of environmentally harmful chemicals.

PEG-like structures have been synthesized by cold plasma technology. Under cold plasma environments, PEG-like structures can be generated directly by fragmenting the appropriate starting volatile chemicals. Denes and colleagues<sup>21</sup> reported the presence of PEG-like structure on stainless steel surfaces by fragmenting 12-crown-4-ether or tri(ethylene glycol) dimethyl-ether (triglyme) using cold plasma, and the resulting surfaces showed significantly reduced bacterial attachment and biofilm formation by mixed cultures of *Salmonella* Typhimurium, *Staphylococcus epidermidis*, and *Pseudomonas fluorescens*. Wang and coworkers used di(ethylene glycol) vinyl ether cold plasma to generate PEG-like structure and observed 81–97% decrease of *Listeria monocytogenes* attachment and biofilm formation on plasma treated stainless steel.<sup>22</sup> These methods provided a very simple and efficient way to generate PEG-like structures, except that the starting chemicals selected might be toxic. With the exception of the previous mentioned, considerably less work has been done on the area of PEG-modified metal surfaces (like stainless steel) oriented to the prevention of bacterial attachment and biofilm formation.

In this study we used cold plasma to crosslink the spin-coated PEG to generate antifouling thin layers onto SS surfaces. PEG films were produced by spin coating the polymer from volatile solvents, and argon radio frequency (RF)-plasma was applied to the spin-coated PEG films to induce crosslinking and thus to reduce its natural solubility. SS, which is a commonly used material in the food processing industry because of its anticorrosion and mechanic properties, was selected as the substrate. *Listeria monocytogenes*, due to its ubiquitous nature and potential of causing severe foodborne disease, was used to evaluate the antifouling abilities of PEG-modified surfaces.

## EXPERIMENTAL

### Materials

SS, type 304, #4 finish (SS #4) and #8 finish (SS #8), were obtained from Temperature Systems (Madison, WI) and McMaster-Carr (Chicago, IL), respectively. Chips of 1 cm<sup>2</sup> or 2.54 cm diameter were cut and washed in a hot alkaline detergent (Micro; International Products, Trenton, NJ) for 30 min, rinsed in

distilled water, air-dried at room temperature, and stored in a sealed petri dish for future use. Control chips that were not plasma-modified were sterilized by autoclaving before bacterial attachment and biofilm formation studies. PEG (MW 400 and 2000) was purchased from Aldrich Chemical Company (Milwaukee, WI). Argon and oxygen supplied by Liquid Carbonic (Milwaukee, WI) were used for decontamination of the plasma reactor, as well as plasma modification.

### Spin coating and plasma processing

All plasma reactions were performed in a parallel plate, capacitively coupled (20 cm diameter SS disc-shaped electrodes; gap between the electrodes, 3 cm; grounded lower electrode) cylindrical SS reactor described previously.<sup>21</sup> The reactor is equipped with a 13.56 MHz RF power supply. Plasma experiments were preceded by a 10 min oxygen plasma (300 W, 300mTorr) cleaning procedure to remove possible contaminants from earlier plasma reactions.

All SS surfaces were oxidized by oxygen plasma before PEG modification. In a typical experiment, clean SS substrates were placed on the lower electrode, and then the reaction chamber was closed and evacuated to base pressure. The preselected oxygen working pressure (300 mTorr) was established in the reactor by operating the needle valve system and the large capacity valve. The plasma state was then initiated by dissipating RF-power (300 W) to the electrodes and sustained for 5 min. This plasma-oxidation step was required to improve the hydrophilicity of the SS substrates. At the end of the reaction, the chamber was evacuated to base pressure, followed by re-pressurizing the system to atmospheric conditions. For PEG400 modification, both sides of the substrates were oxidized by oxygen plasma. Samples were then removed for spin coating with PEG.

A single 6 in. wafer spin processor WS-400A-6NPP/Lite (spin coater) from Laurell Technologies Co. (North Wales, PA) with time, speed (up to 6000 rpm), and acceleration/deceleration programmable in multiple steps per program was employed for the deposition of PEG thin layers from ethanol or ethanol-water solutions. PEG400 is a viscous liquid and can be dissolved easily in ethanol. The spinning program was first set at 6000 rpm for 20 s. Preliminary testing with different concentrations of PEG400 (1–10%) indicated that 3% gave the most stable PEG film after plasma crosslinking. This concentration was, therefore, used for all subsequent experiments with PEG400. SS #4 samples of 1 cm<sup>2</sup> were used, and 20  $\mu$ L of the PEG400 solution was placed on the surfaces before spinning.

PEG2000 is a wax-like solid and cannot be dissolved in absolute ethanol but dissolves in 95% ethanol-water solution. Because surface topography is thought to play an important role in bacterial attachment,<sup>23</sup> we

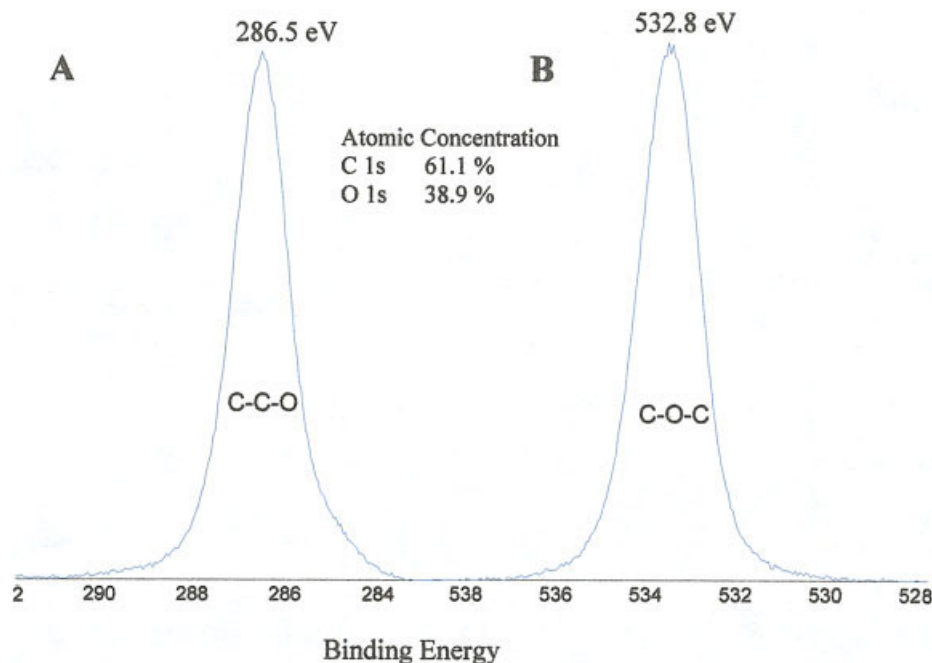


**Figure 1** High resolution (A) C1s and (B) O1s ESCA spectra of PEG400. Color figure can be viewed in the online issue, which is available at [www.interscience.wiley.com](http://www.interscience.wiley.com).

wanted to compare the effect of different roughness on bacterial attachment as well as plasma treatment. For this purpose, SS #8, which has a much smoother surface than SS #4, was also used for PEG2000 modification. Spin coating on SS #8 indicated that round samples gave a more uniform PEG film; therefore, round samples of 2.54cm diameter were cut and 100  $\mu$ L of the PEG2000 solution was used for spin coating. However, PEG2000 films spin-coated on SS #8 chips at 6000 rpm for 20 s (parameters used for SS #4 with PEG400 modification) turned out to be very nonuniform. By experimenting with different spin speeds and spin times, PEG2000 spun at 3000 rpm for 15 s gave a very uniform PEG film on SS #8 chips. PEG2000 films spin-coated from a 3% solution at this condition were not stable on SS #8 chips with the same plasma modification parameters used for PEG400. When a lower concentration (1%) of PEG2000 was spin-coated at 3000 rpm for 15 s, a uniform and stable film could be achieved after appropriate plasma modification. This concentration (1%) and spin condition (3000 rpm, 15 s) were, therefore, used in all the experiments with PEG2000 modification on round SS #4 and SS #8 chips.

The spin-coated SS samples were immediately crosslinked by argon plasma. The chips were positioned on the lower electrode of the plasma reactor and processed under the following plasma parameters: plasma gas, argon; base pressure in the reactor, 30 mTorr; pressure in the presence of plasma, 150–200 mTorr; RF-power dissipated to the electrodes, 50 W, 100 W, or 150 W; treatment time, 30 s, 1 min, or 2 min; temperature of the reactor, 25°C. The plasma-modified

substrates were then removed, rinsed with distilled water to remove unbound PEG, vacuum dried for half an hour at room temperature, and stored in clean sterile petri dishes. For PEG400-modified SS #4, the spin coating and argon plasma crosslinking procedure was repeated on the other side of the samples.

#### Stability of the PEG-modified SS surfaces

To test the stability of plasma-modified PEG films on SS surfaces, SS chips were put into flasks containing 25 mL 10 mM sodium phosphate-buffered saline (PBS, pH 7.2) and incubated at 27°C at 100 rpm in a water bath shaker for 48 h. The samples were removed, rinsed with distilled water three times, and air dried for ESCA analysis.

#### Analytical methods

Survey and high resolution electron spectroscopy for chemical analysis (ESCA) of unmodified and PEG-modified SS substrates were performed with a Perkin-Elmer Physical Electronics 5400 Small Area Spectrometer (Mg source; 15 kV; 300 W; pass energy, 89.45 eV; take-off angle, 45°; Perkin-Elmer, Palo Alto, CA). To correct for surface-charge-origin binding energy shifts, calibrations were performed based on the well-known C-C-C (285 eV) and C-C-O (286.5 eV) peaks.

Attenuated total reflectance-Fourier transform infrared spectroscopy (ATR-FTIR) was used to identify the chemical linkages on the PEG-modified surfaces. An ATI-Mattson Research Series IR instrument pro-

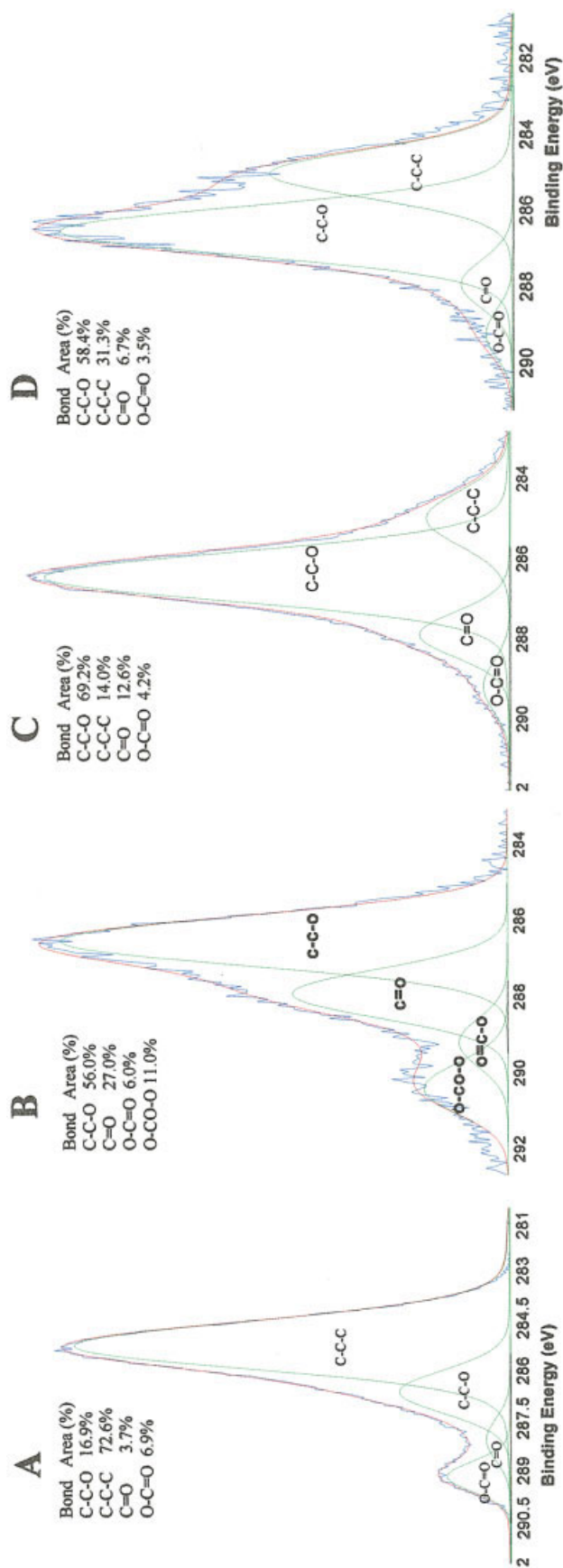


**Figure 2** High resolution C1s ESCA spectra of SS #4 (A) unmodified, (B) oxygen plasma modified at 300W-5min, (C) PEG400 modified by Ar plasma at 100W-1min, and (D) PEG2000 modified by Ar plasma at 50W-1min. Color figure can be viewed in the online issue, which is available at [www.interscience.wiley.com](http://www.interscience.wiley.com).

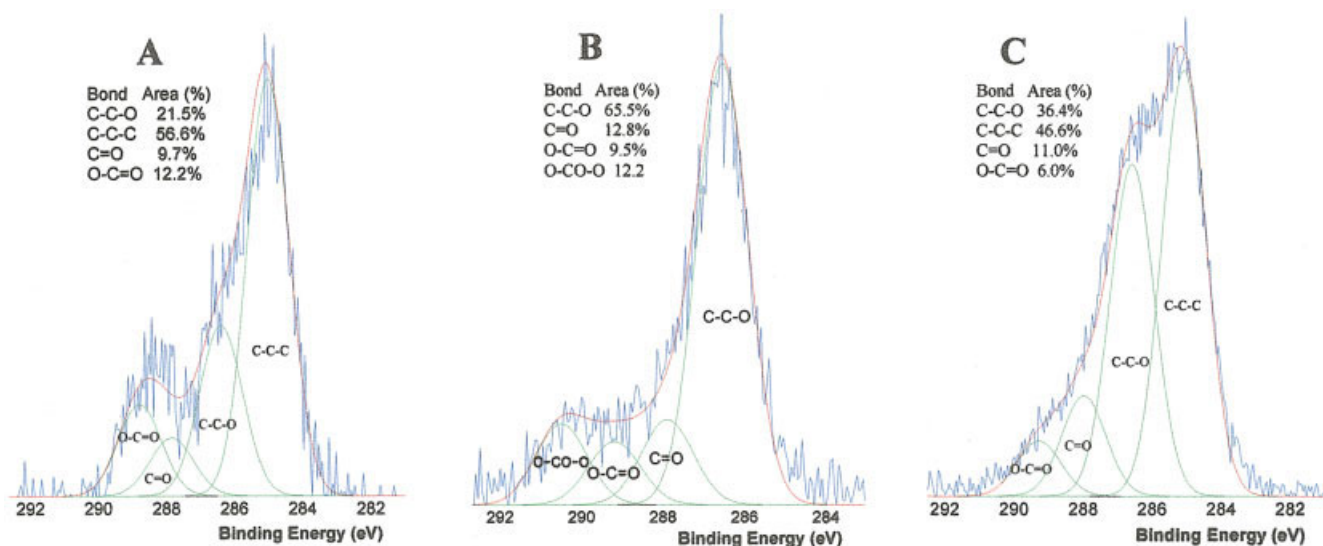


**Figure 3** High resolution C1s ESCA spectra of SS #8 (A) unmodified, (B) oxygen plasma modified at 300W-5min, and (C) PEG2000 modified by Ar plasma at 50W-1min. Color figure can be viewed in the online issue, which is available at [www.interscience.wiley.com](http://www.interscience.wiley.com).

vided with a GRASEBY-Special Benchmark series ATR in-compartment P/N/11,160 unit (Mattson Instruments, Madison, WI) was used. All ATR-FTIR evaluations were performed under a nitrogen blanket generated from a flow-controlled liquid nitrogen tank. Data acquisition consisted of 250 scans in the 600–4000 wave number region. ATR-FTIR reveals information from surface layers as thick as 10–15  $\mu\text{m}$ , and cold-plasma-induced surface functionalization reactions only involve the top 100  $\text{\AA}$  surface layers, which means the unmodified bulk volume of the samples will dominate the IR signatures. Therefore, potassium bromide (KBr; Aldrich Chemical Company, Milwaukee, WI) pellets, made with a Carver Laboratory Press (Fred S. Carver Inc., Wabash, IN), were used for sample mounting. KBr powder was ground on the surface of samples after both were dried in a vacuum oven. About 0.6 g KBr powder was used per pellet. Differential spectra resulting from the subtraction of reference spectra (untreated substrate) from the spectra of the PEG-modified samples were analyzed.

Surface topographies of unmodified and PEG-modified SS surfaces were evaluated by contact mode atomic force microscopy (AFM; Pico Scan, Molecular Imaging Inc. Tempe, AZ) with: scanner area, 6  $\mu\text{m}^2$ ; scan rate, 5147.9/s; data points per line, 512; silicon nitride nanoprobe.

Surface roughness was compared based on the mean absolute deviation value (MAD), which was calculated using the formula:

$$MAD = \frac{1}{N} \sum_{i=1}^N f_i |x_i - \bar{x}|$$

where N is the number of points within the given area,  $f_i$  is the number of data points that fall within the given area in a frequency distribution,  $x_i$  is the current difference between the highest and the lowest points, and  $\bar{x}$  is the average of the values with the given area. Flattening was done to remove the curvatures of samples. For each treatment, five 6- $\mu\text{m}^2$  areas from each of three triplicate samples were scanned and average MAD was calculated.

Scanning electron microscopy (SEM; LEO 1530 field emission, LEO Electron Microscopy Inc., Thornwood, NY) was also used to analyze surface morphologies. For SEM analysis, the substrates were gold-sputter coated in a Desk II system sputter coater (Denton Vacuum Inc., Moorestown, NJ) at 50mTorr and 45mA for 30s.

Contact angle evaluations were performed using a manual goniometer (Ramé-Hart, Inc., Model 100–00-115, Mountain Lakes, NJ). Water droplets of 5  $\mu\text{L}$  were used in each measurement, and a minimum of 10 readings per sample were made.

### Bacterial attachment and biofilm formation

Both bacterial attachment and biofilm formation of unmodified and PEG-modified SS surfaces were evaluated. Five strains of *L. monocytogenes*, Scott A (serotype 4b, human isolate), JBL 1157 (serotype 4b, processed meat), CLIP 23,485 (unknown serotype, liver pâté), F6900 (serotype 1/2a, human), and F8964 (serotype 1/2b, human) were used. The strains were grown individually for 24 h in 5 mL trypticase soy broth (TSB; BBL Microbiology Systems/Becton Dickinson, Cockeysville, MD) at 37°C, and then 500  $\mu\text{L}$  from each

culture were combined to form a 5-strain cocktail. A 100  $\mu$ L portion of the cocktail was transferred to a sterile 250 mL flask containing 50 mL extracellular polysaccharide (EPS) medium with yeast extract<sup>21</sup> to achieve an initial bacterial concentration of  $10^6$  colony-forming units (CFU)/mL. For biofilm development, SS chips were placed inside the flasks after inoculation, and the cultures were incubated at 27°C at 100 rpm in a gyratory water bath shaker (model G76, New Brunswick Scientific, Edison, NJ) for 48 h. For attachment studies, the inoculated cultures were incubated at 27°C at 100 rpm for 6h, SS chips were placed inside the flasks, and the cultures were then incubated for another 1 h.

After 1h attachment or 2 days biofilm formation, SS chips were aseptically removed from the flasks and put in a petri dish containing 25 mL PBS. The chips were rinsed by manually rotating the petri dish 10 times clockwise and 10 times counterclockwise to remove unattached bacteria. The chips were removed, put in a tube containing 4.5 mL PBS with glass beads, and vortexed for 30 s to remove bacteria from the surfaces. The number of organisms was evaluated by plating appropriate dilutions onto brain heart infusion agar (Difco/Becton Dickinson, Sparks, MD) plates. The plates were incubated at 30°C for 48 h, and the numbers of CFUs developed were counted. This method of bacteria recovery was only used for 1 cm<sup>2</sup> SS #4 chips that had been modified with PEG400. In each experiment, two SS chips were used for each tested condition. Data were collected from at least four independent experiments.

With PEG2000, round SS #4 and SS #8 chips of 2.54 cm diameter were used, and only one side was spin-coated and plasma treated. Epifluorescence microscopy was used to enumerate the number of attached bacteria on these samples. The incubation of samples was the same as described above for 1 cm<sup>2</sup> chips, except that 600 mL beakers were used instead of 250 mL flasks to accommodate the larger chips. After 1h attachment or 2 days biofilm formation, samples were removed from beakers and rinsed with PBS. To fix the bacteria on the surfaces, chips were soaked in 20 mL 1% glutaraldehyde for 30 min and then rinsed twice with distilled water. Attached bacteria were stained with acridine orange (0.025% in 0.026M citric acid buffer, pH6.6) (Sigma, St. Louis, MO) for 5 min, rinsed twice with distilled water, and then air dried. Cells were enumerated using the oil immersion objective (100 $\times$ ) and a 10 $\times$  ocular lens on a Carl Zeiss Standard Microscope equipped for epifluorescence with an HB050 mercury light source and the Zeiss 09 filter combination (excitor AP450–490; reflector FT510; barrier filter LP520). The microscopic field (0.03 mm<sup>2</sup>) was measured by a stage micrometer, and 20 representative fields per chip were recorded. The cells per cm<sup>2</sup> were calculated and transformed into log cells per

cm<sup>2</sup>. Duplicate chips were used for each testing condition, and data were collected from at least four independent experiments.

### Statistics

Data were analyzed with Student's *t*-test; differences were considered statistically significant at  $p < 0.05$ .

## RESULTS AND DISCUSSION

### Surface chemistry of unmodified and PEG-modified surfaces

#### ESCA analysis

Pure PEG400, spin-coated onto a plasma oxidized SS surface, was analyzed by ESCA. The high resolution C1s and O1s ESCA spectra and the relative surface atomic concentrations of PEG400 are presented in Figure 1. Only very symmetric C–C–O (286.5 eV) and C–O–C (532.8 eV) peaks were present in the C1s and O1s spectra, respectively. The relative C/O ratio is 1.6, which is lower than the theoretical value of 2.0 according to the structure of PEG. Because PEG is very hygroscopic, the absorption of moisture might contribute to the decrease in the observed value.

It is important to note that even thoroughly cleaned, unmodified SS samples retain on their surfaces an environmentally acquired thin oxidized carbon layer. Similar results have been reported by other studies.<sup>9,22</sup> The high resolution C1s ESCA spectra of unmodified SS #4 (Fig. 2A) and #8 (Fig. 3A) indicated the presence of a dominant C–C–C binding energy peak (285 eV) accompanied by low surface areas of C–C–O (286.5 eV), C=O (288 eV), and O–C = O (289.2 eV) peaks. Survey ESCA data showed the presence of a significant amount of carbon and oxygen and relatively low iron (C/O = 1.30, 2.1% of Fe2p for SS #4; C/O = 0.76, 3.7% of Fe2p for SS #8) on SS substrates. The higher C/O ratio might contribute to the higher hydrophobicity of SS #4 than SS #8, as observed later by the water contact angles.

The surface structure of SS was significantly modified after oxygen plasma treatment. The significantly decreased C/O ratio (C/O = 0.45 for SS #4; C/O = 0.38 for SS #8) indicated that an intense oxidation had occurred. During oxygen plasma treatment, dissociation of C–C and C–H occurred, and oxygen was subsequently incorporated into the surface. A slightly increased iron level (7.9% in oxidized SS #4 and 5.9% in oxidized SS #8) might be the result of the simultaneous plasma-induced oxidation and etching. For both oxidized SS #4 (Fig. 2B) and SS #8 (Fig. 3B), the high resolution C1s ESCA spectra showed the appearance of an O–CO–O (290.5 eV) binding energy peak, increased surface area of C–O and C=O peaks, and disappearance of the C–C–C peak. In addition to en-

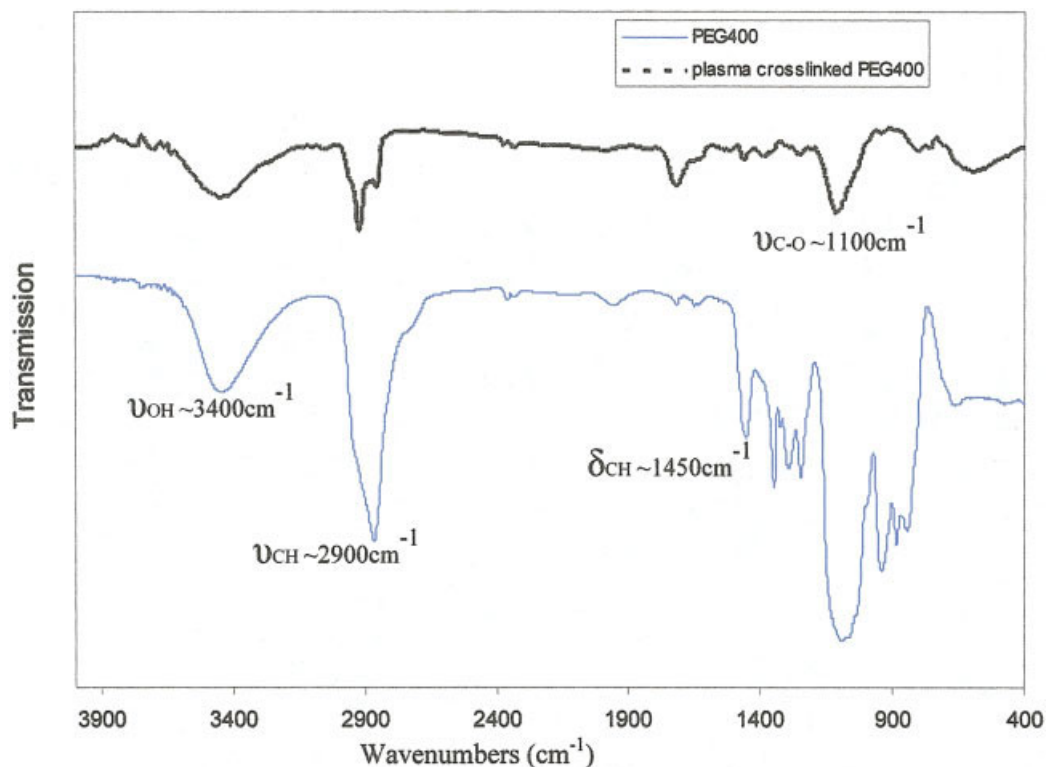


**Figure 4** ATR-FTIR spectra of liquid-phase PEG400 and argon plasma-modified PEG400. Color figure can be viewed in the online issue, which is available at [www.interscience.wiley.com](http://www.interscience.wiley.com).

hancing wettability, in an argon plasma environment these active species on the surface can be utilized to mediate the interaction between the SS surface and PEG molecules, thus keeping the polymerized PEG stable on SS surfaces.

Different plasma power levels (50 W, 100 W, 150 W) and exposure times (30 s, 1 min, 2 min) were used to crosslink PEG400 spin-coated on SS #4 surfaces. Stability of the PEG film crosslinked by various plasma parameters was tested in PBS. If the crosslinking process was insufficient, the deposited PEG film would be soluble in PBS. Films spin-coated with 3% PEG400 and treated by argon plasma at 100 W for either 1 or 2 min gave the most stable films, and similar ESCA results were obtained. The high resolution C1s ESCA spectra of argon-plasma crosslinked PEG400 for 1 min (2 min not shown) on SS #4 showed a dominant C-C-O peak, smaller C=O and O-C=O peaks, and the presence of a C-C-C peak (Fig. 2C). As proposed by Manso and coworkers,<sup>24</sup> if a C-O bond and a neighboring C-C bond are broken by incident argon ions, crosslinking of PEG molecules could result as the two dangling bonds form a propylene center. The reappearance of a C-C-C peak and the predominant presence of the C-C-O peak are strong evidence that the PEG400 film was successfully crosslinked. The disappearance of the iron signal in the survey ESCA spectra (data not shown) and a highly oxidized O-CO-O peak in the

high resolution C1s spectrum suggest that the surface has been completely covered by the crosslinked PEG film. The uniform coverage of the PEG400 film was verified by similar ESCA spectra obtained from random locations on the same sample surface.

The same argon plasma parameters were used to test the crosslinking of spin-coated PEG2000 films (from 1%) on SS #4. Plasma condition of 50 W and 1 min was selected as optimal (most stable; high C-C-O peak). Compared with the C1s ESCA spectra of PEG400-modified SS #4, the PEG2000-modified SS #4 (Fig. 2D) had the same four characteristic bonding peaks but a larger surface area C-C-C peak, indicating a more intense crosslinking process had occurred during PEG2000 modification. Undetectable iron signal and the disappearance of the highly oxidized O-CO-O peak were an indicator of complete coverage after PEG2000 modification.

The same optimal plasma condition (50 W, 1 min) was selected for crosslinking of PEG2000 (from 1%) on SS #8 from preliminary testing. The C1s ESCA spectrum of PEG2000-modified SS #8 surfaces showed a larger C-C-C peak area than the C-C-O peak (Fig. 3C) and the C-C-C peak of PEG2000-modified SS #4, suggesting that the crosslinking of PEG2000 was more intense on smoother SS surfaces, which is in agreement with our hypothesis that surface roughness has an influence on plasma treatment. Complete coverage

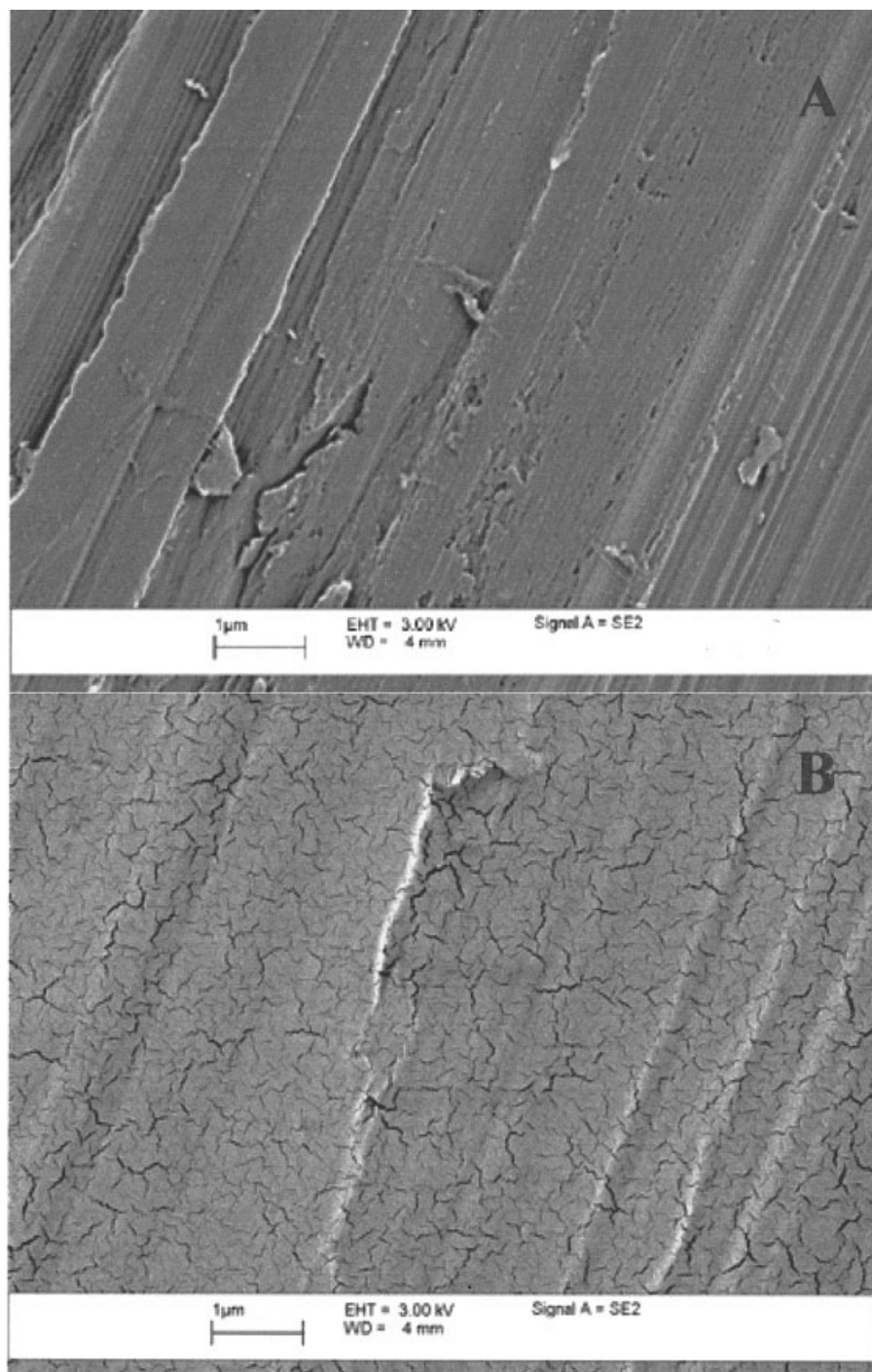


**Figure 5** SEM images of (A) unmodified and (B) PEG400 modified SS #4.

of the crosslinked PEG2000 film was confirmed by undetectable iron signal and disappearance of the highly oxidized O-CO-O peak from the C1s spectrum.

#### ATR-FTIR

Typical ATR-FTIR spectra of liquid-phase PEG400 and PEG400 crosslinked by argon plasma on SS #4 are presented in Figure 4. The characteristic vibrations of

pure PEG400 including OH stretching ( $\sim 3400\text{ cm}^{-1}$ ), CH<sub>2</sub> stretching ( $\sim 2900\text{ cm}^{-1}$ ), CH deformation from CH<sub>2</sub> ( $\sim 1450\text{ cm}^{-1}$ ), and C-O stretching ( $\sim 1100\text{ cm}^{-1}$ ) were also present in the IR spectrum of plasma-modified PEG400. In addition, relatively increased absorption bands around 1650 and 2800  $\text{cm}^{-1}$  were observed, which might be related to the unsaturated structures including hydrocarbon-type linkages, ketones, and aldehydes as a result of crosslinking. The intensity of the



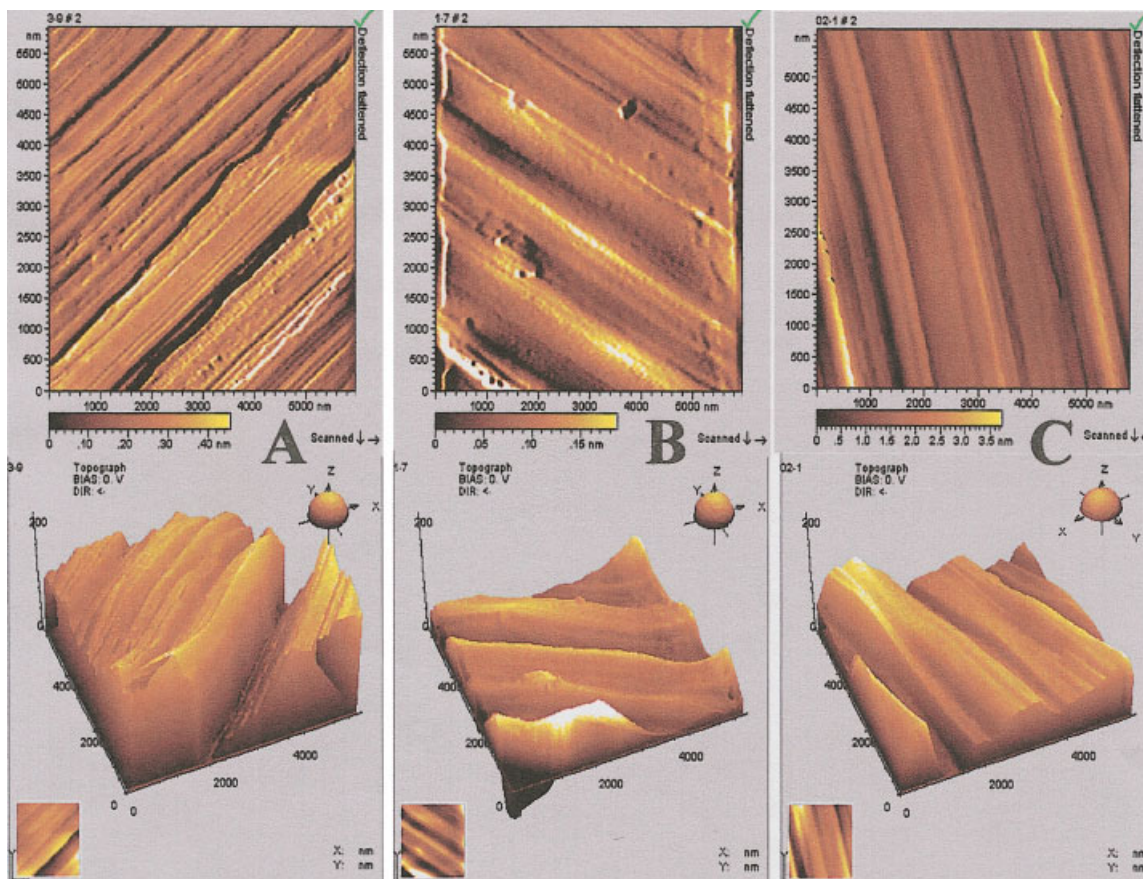


**Figure 6** AFM top view and 3D images of (A) unmodified, (B) PEG400-modified, and (C) PEG2000-modified SS #4. Color figure can be viewed in the online issue, which is available at [www.interscience.wiley.com](http://www.interscience.wiley.com).

CH<sub>2</sub> and C-O absorption bands on plasma-modified PEG400 decreased more relative to the OH absorption band, which suggests that a different hydrogen-bonding process was associated with plasma-mediated crosslinking. Overall, the ATR-FTIR spectra substantiated the ESCA data that PEG400 was successfully crosslinked by argon plasma.

### Surface morphology

#### SEM

The surfaces of unmodified and PEG-modified SS were examined by SEM, which indicated that the SS surfaces were completely coated after PEG modification. Representative high magnification (40K) SEM images of unmodified and PEG400-modified SS #4 are shown in Figure 5. The presence of a crack-array pattern on the modified surfaces might have resulted from the gold-sputtering during sample preparation for SEM analysis.<sup>22</sup> Similar patterns were also identified on PEG2000 modified SS #4 and SS #8 substrates (images not shown). Alternatively, the "crack" might be due to dehydration and shrinkage of the normally hydrated PEG. It has been shown that the hydrated

extracellular polysaccharide (EPS) layer of biofilm is seen in SEM images as condensed or stringy layers due to the dehydration steps used to prepare the samples.<sup>25</sup>

#### AFM

AFM images and surface roughness measurements collected from unmodified and PEG-modified SS samples substantiated the results from SEM that a smoother surface coating was present on the PEG-modified SS surfaces in comparison to the unmodified substrates ( $p < 0.05$ ) (Figs. 6–8). This could be explained by the presence of a deposited layer, which covered some of the grooves on the original surface. Surface roughness was measured by mean absolute deviation (MAD), which is equivalent to the commonly used average roughness (Ra). Flattening was done to remove the curvature of samples, and a small area of 6  $\mu\text{m}^2$  was scanned. This might explain the smaller MAD values (MAD = 313 Å) we recorded compared to Ra values for SS #4 reported by others. The unmodified SS #8 was much smoother (MAD = 31 Å) than unmodified SS #4. The oxygen plasma

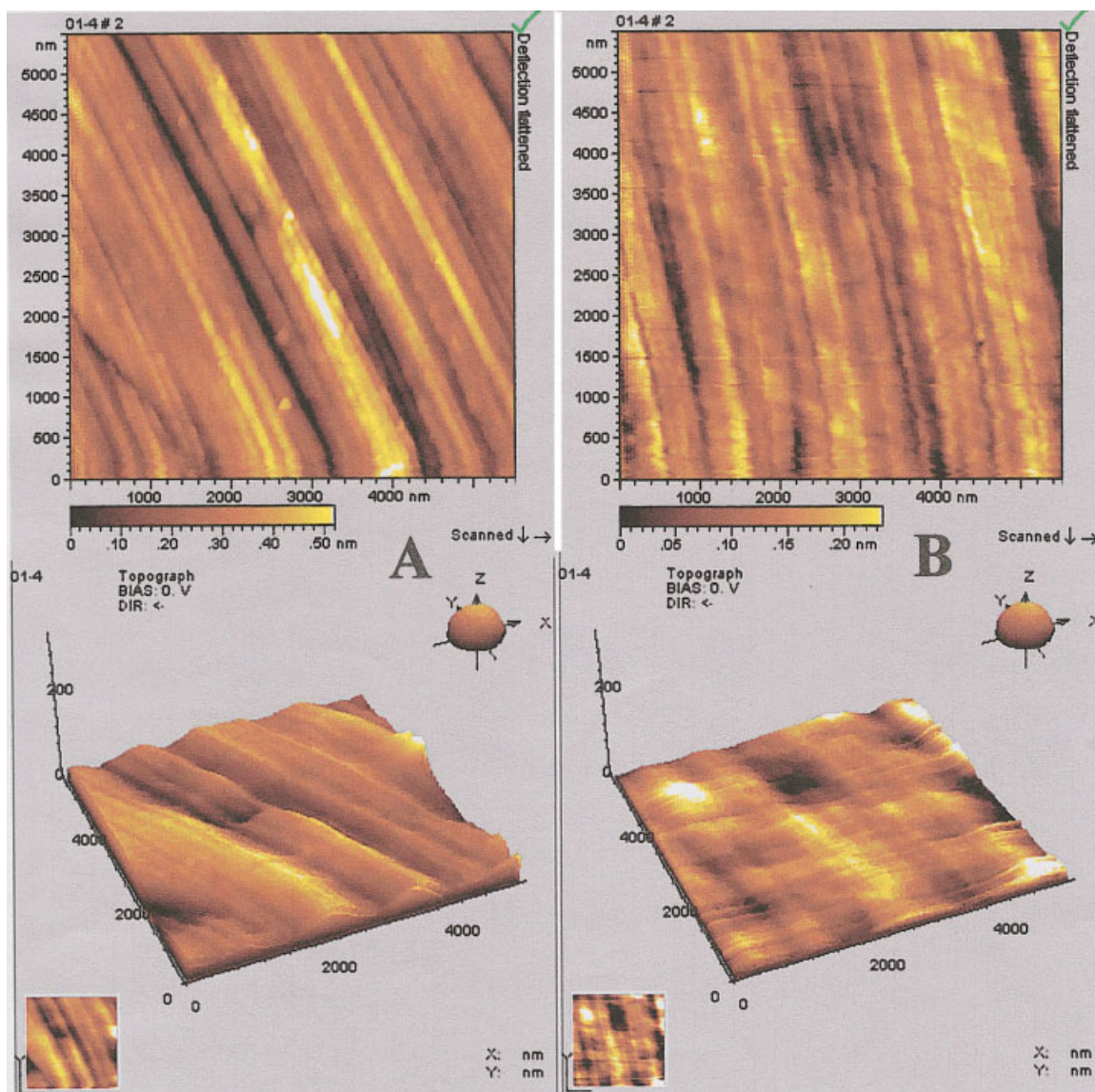


**Figure 7** AFM top view and 3D images of (A) unmodified and (B) PEG2000-modified SS #8. Color figure can be viewed in the online issue, which is available at [www.interscience.wiley.com](http://www.interscience.wiley.com).

oxidation process did not change significantly the surface roughness of SS surfaces, as demonstrated by MAD values similar to those for their corresponding unmodified controls.

#### Water contact angle

The water contact angle values of unmodified and plasma-modified SS surfaces are shown in Figure 9. The contact angle for unmodified SS #4 is  $74^\circ$ , which is lower than the reported value of  $85\text{--}86^\circ$ .<sup>22,26</sup> Instrument variation and different sample orientation might be related to the difference. A contact angle of  $52^\circ$  was recorded for unmodified SS #8, which had a lower surface C/O ratio than that of unmodified SS #4. As

expected, oxygen plasma treated SS samples had very hydrophilic surfaces, as demonstrated by the low contact angles ( $15^\circ$  for oxidized SS #4;  $17^\circ$  for oxidized SS #8). The relatively high oxygen composition and formation of polar functional groups (C-O, C=O) as a result of oxygen plasma exposure could contribute to the low contact angles. The PEG-modified surfaces were more hydrophilic compared with their respective unmodified surfaces, but less hydrophilic than the oxidized SS surfaces. The ability of PEG structures to form hydrogen bonds with water could explain the increased hydrophilicity compared to the unmodified surfaces, which has been hypothesized to be partially responsible for the antifouling ability of PEG-type structures.<sup>27</sup>

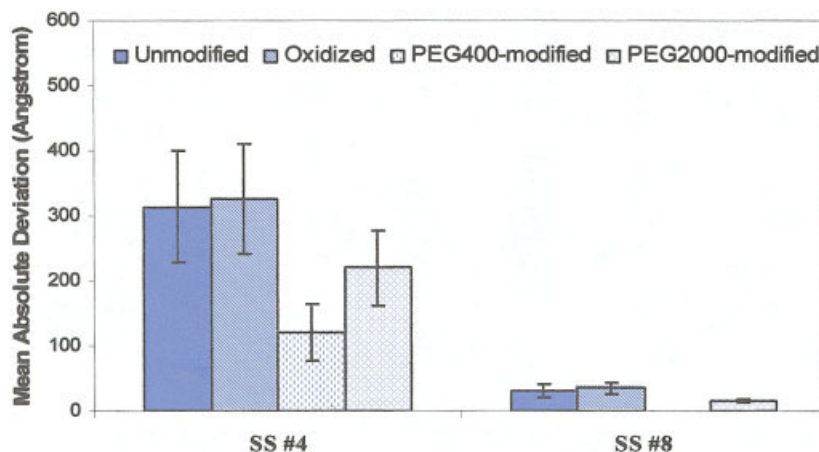


**Figure 8** Surface roughness of unmodified and plasma-modified SS surfaces. Color figure can be viewed in the online issue, which is available at [www.interscience.wiley.com](http://www.interscience.wiley.com).

#### Antifouling evaluation by bacterial attachment and biofilm formation

SS #4 modified with PEG400 decreased *L. monocytogenes* attachment by 96%, whereas biofilm formation was reduced by 81%, compared with the unmodified SS #4 (Fig. 10). All decreases observed were statistically significant ( $p < 0.05$ ). It is worthy of note that the biofilm results from oxygen plasma treated SS #4 were the same as the unmodified SS #4, although the oxidized SS #4 had a larger C-C-O peak area and significantly lower water contact angle. This suggests that the decrease observed was due to the deposition of crosslinked PEG400. Denes and coworkers<sup>21</sup> have reported an increased bacterial attachment and biofilm formation on plasma oxidized SS304 by *Salmonella* Typhimurium, *Staphylococcus epidermidis*, and *Pseudo-*

*monas fluorescens*. The difference could be the result of different bacteria used and different oxygen plasma parameters applied.

Representative epifluorescence microscopy images of attachment on unmodified and PEG2000-modified SS are shown in Figure 11. Attachment of *L. monocytogenes* was reduced by 84 and 88%, whereas biofilm formation was reduced by 86 and 87% on PEG2000-modified SS #4 and SS #8, respectively, compared to the unmodified controls ( $p < 0.05$ ) (Fig. 12). There was no significant difference between the SS #4 and SS #8 of PEG2000-modified surfaces with respect to attachment and biofilm formation. PEG2000-modified SS #4 had a higher C-C-O peak area and lower water contact angle compared to PEG2000-modified SS #8, which could help reduce the adherence of bacteria; PEG2000-

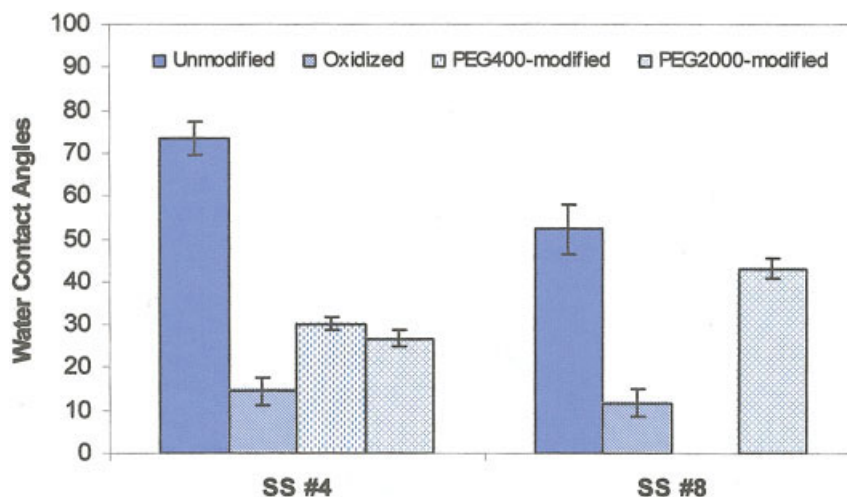


**Figure 9** Water contact angles of unmodified and plasma modified SS surfaces. Color figure can be viewed in the online issue, which is available at [www.interscience.wiley.com](http://www.interscience.wiley.com).

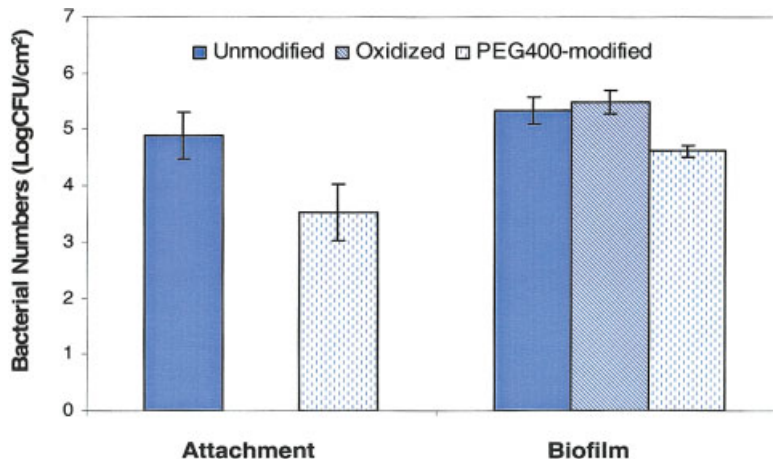


**Figure 10** Bacteria attachment and biofilm formation by *L. monocytogenes* of unmodified and PEG400-modified SS #4. Color figure can be viewed in the online issue, which is available at [www.interscience.wiley.com](http://www.interscience.wiley.com).

modified SS #4 had rougher surfaces, and it has been shown that rougher surfaces could increase adhesion of microorganisms.<sup>28</sup>

Most studies using PEG-modified surfaces or surfaces with PEG-like structures were focused on enhancing biocompatibility and showed significantly reduced protein adsorption; only a few studies were related to bacterial attachment. Moreover, very few people used SS as a substrate for modification. Wei

and colleagues<sup>29</sup> demonstrated that PEG was successfully grafted onto poly(ethylenimine) immobilized SS surfaces, whereas no decrease in bacterial adhesion either by *Pseudomonas* sp. or by *L. monocytogenes* was observed. Our results are in agreement with those reported for di(ethylene glycol) vinyl ether plasma treated SS, which had PEG-like structures and reduced the attachment and biofilm formation by *L. monocytogenes*.<sup>22</sup>

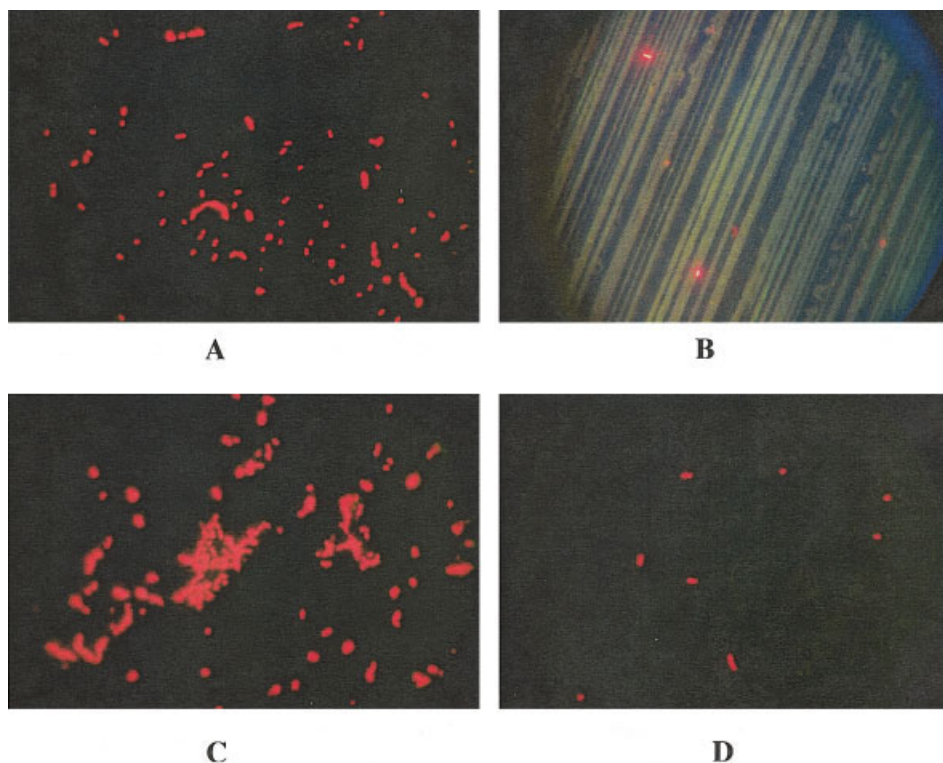


**Figure 11** Epifluorescence images of 1 h attachment of (A) unmodified and (B) PEG2000-modified SS #4, and (C) unmodified and (D) PEG2000-modified SS #8. Color figure can be viewed in the online issue, which is available at [www.interscience.wiley.com](http://www.interscience.wiley.com).

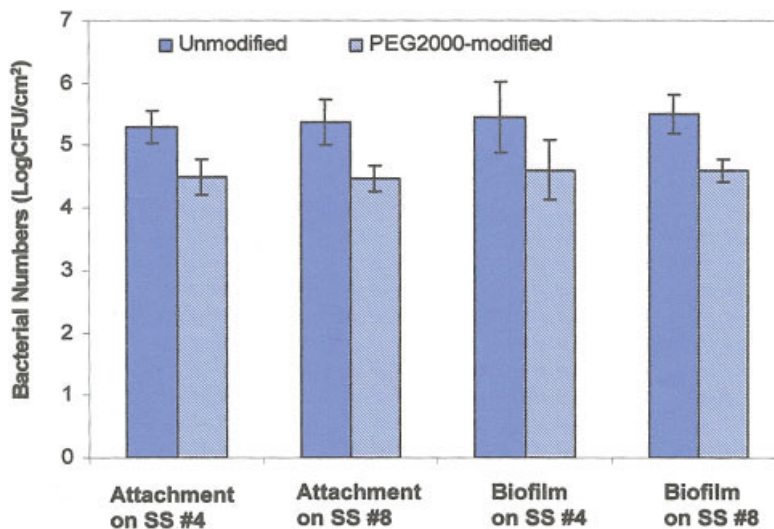


**Figure 12** Bacteria attachment and biofilm formation by *L. monocytogenes* on unmodified and PEG2000-modified SS #4 and SS #8. Color figure can be viewed in the online issue, which is available at [www.interscience.wiley.com](http://www.interscience.wiley.com).

## CONCLUSIONS

Thin spin-coated PEG films were stabilized by crosslinking on SS surfaces with argon plasma, as demonstrated by the presence of C-C-O and C-C-C as the main linkages with ESCA analysis. Surface morphology evaluations indicated the presence of uniform and smooth depositions on PEG-modified SS surfaces. Significantly reduced attachment and biofilm formation by *L. monocytogenes* was observed on all PEG-modified SS surfaces.

This plasma technology provided a very efficient way for the deposition of stable PEG structures on metal surfaces like SS. In addition to SS, this approach could be applied to other materials, such as silicone rubber (undergoing), polyester, expanded polytetrafluoroethylene (ePTFE), and other polymeric materials. In the case of substrates with hydrophilic surfaces, oxygen plasma oxidation treatment may not be necessary since complete coverage might be obtained directly from spin coating of PEG on the substrate. Compared with other methods used to produce PEG-containing surfaces, this cold plasma-mediated crosslinking method is easy and does not involve the usage of bulk toxic reagents. This provides an alternative strategy for generating antifouling layers for food processing and biomedical applications.

## References

- Bott, T. R.; Melo, L. F.; Fletcher, M.; Capdeville, B. *Biofilms Science and Technology*; Kluwer Academic Press: Dordrecht, The Netherlands, 1992; p 3.
- Carpentier, B.; Cerf, O. *J Appl Bacteriol* 1993, 75, 499.
- Russell, P. *Milk Industry* 1993, 95, 10.
- Zottola, E. A.; Sasahara, K. C. *Int J Food Microbiol* 1994, 23, 125.
- Kumar, C. G.; Anand, S. K. *Int J Food Microbiol* 1998, 42, 9.
- Costerton, J. W.; Lewandowski, Z.; Caldwell, D. E.; Korber, D. R.; Lappin-Scott, H. M. *Ann Rev Microbiol* 1995, 49, 711.
- Characklis, W. G. In *Biofilms*; Characklis, W. G.; Marshall, K. C., Eds.; Wiley: New York, 1990; p 195.
- Scott, K. H.; Edmund, A. Z. *Int J Food Microbiol* 1997, 37, 145.
- Zhang, F.; Kang, E. T.; Neoh, K. G.; Wang, P.; Tan, K. L. *Biomaterials* 2001, 22, 1541.
- Kiss, E.; Samu, J.; Toth, A.; Bertoti, I. *Langmuir* 1996, 12, 1651.
- Gombotz, W. R.; Guanghui, W.; Horbett, T. A.; Hoffman, A. S. *J Biomed Mater* 1991, 25, 1547.
- Alcantar, N. A.; Aydil, E. S.; Israelachvili, J. N. *J Biomed Mater Res* 2000, 51, 343.
- Zhang, Q.; Wang, C. R.; Babukutty, Y.; Ohshima, T.; Kogoma, M.; Kodama, M. *J Biomed Mater Res* 2002, 60, 502.
- Akizawa, T.; Kino, K.; Koshikawa, S.; Ikada, Y.; Kishida, A.; Yamashita, M.; Imamura, K. *Trans Am Soc Artif Intern Organs* 1989, 35, 333.
- Amiji, M.; Park, P. *J Biomater Sci Polym Ed* 1993, 4, 217.
- Brinkman, E.; Poot, A.; Does, V. D. L.; Bantjes, A. *Biomaterials* 1990, 11, 200.
- Sun, Y. H.; Gombotz, W. R.; Hoffman, A. S. *J Bioactive Compat Polym* 1986, 1, 316.
- Zhang, M.; Desai, T.; Ferrari, M. *Biomaterials* 1998, 19, 953.
- Lee, J. H.; Lee, H. B.; Andrade, J. D. *Prog Polym Sci* 1995, 20, 1043.
- Park, K. D.; Kim, Y. S.; Han, D. K.; Kim, Y. H.; Lee, E. H. B.; Suh, H.; Choi, K. S. *Biomaterials* 1998, 19, 851.
- Denes, A. R.; Somers, E. B.; Wong, A. C. L.; Denes, F. S. *J Appl Polym Sci* 2001, 81, 3425.
- Wang, Y.; Somers, E. B.; Manolache, S.; Denes, F. S.; Wong, A. C. L. *J Food Sci* 2003, 68, 9.
- Arnold, J. W.; Bailey, G. W. *Poultry Sci* 2000, 79, 1839.
- Manso, M.; Rossini, P.; Malerba, I.; Valsesia, A.; Gribaldo, L.; Ceccone, G.; Rossi, F. *J Biomaterials Sci-Polym Ed* 2004, 15, 161.
- Fassell, T. A.; Edmiston, C. E. *Methods in Enzymol Biofilms*; Academic Press: New York, 1999; p 194.
- Flint, S. H.; Brook, J. D.; Bremer, P. J. *J Food Eng* 2000, 43, 235.
- Wan, S.; Mahmud, N.; Kushner, L.; Lindon, J. N.; Curme, J.; Merrill, E. W.; Salzman, E. W. *Trans Am Soc Artif Intern Organs* 1982, 28, 482.
- Taylor, R. L.; Verran, J.; Lees, G. C.; Ward, A. J. P. *J Mater Sci: Mater Med* 1998, 9, 17.
- Wei, J.; Ravn, B. D.; Gram, L.; Kingshott, P. *Colloids Surf B* 2003, 32, 275.